



UvA-DARE (Digital Academic Repository)

Electrical impedance tomography in high frequency ventilated preterm infants: the search for the Holy Grail

Miedema, M.

Publication date
2011

[Link to publication](#)

Citation for published version (APA):

Miedema, M. (2011). *Electrical impedance tomography in high frequency ventilated preterm infants: the search for the Holy Grail*. [Thesis, fully internal, Universiteit van Amsterdam].

General rights

It is not permitted to download or to forward/distribute the text or part of it without the consent of the author(s) and/or copyright holder(s), other than for strictly personal, individual use, unless the work is under an open content license (like Creative Commons).

Disclaimer/Complaints regulations

If you believe that digital publication of certain material infringes any of your rights or (privacy) interests, please let the Library know, stating your reasons. In case of a legitimate complaint, the Library will make the material inaccessible and/or remove it from the website. Please Ask the Library: <https://uba.uva.nl/en/contact>, or a letter to: Library of the University of Amsterdam, Secretariat, Singel 425, 1012 WP Amsterdam, The Netherlands. You will be contacted as soon as possible.

Changes in lung volume and ventilation during lung recruitment in high frequency ventilated preterm infants with respiratory distress syndrome

Martijn Miedema¹, Frans H de Jongh¹, Inez Frerichs²,
Mariëtte B. van Veenendaal¹, Anton H. van Kaam¹

¹ Department of Neonatology, Emma Children's
Hospital AMC, Amsterdam, The Netherlands

² Department of Anaesthesiology and Intensive Care
Medicine, University Medical Centre Schleswig-
Holstein, Campus Kiel, Germany

Abstract

Objectives: To assess global and regional changes in lung volume and ventilation during lung recruitment in preterm infants with respiratory distress syndrome.

Study design: Using electrical impedance tomography, changes in lung volume and ventilation were measured in 15 high-frequency oscillatory ventilated preterm infants during oxygenation-guided recruitment maneuvers. The inflation and deflation limbs were mapped, and the lower and upper inflection points were calculated using both oxygenation and impedance data. The impedance data were also used to determine recruitment-related changes in oscillation volume and distribution.

Results: During inflation, lower and upper inflection points were identified in the majority of infants. The deflation limb showed clear lung hysteresis in all infants. The upper inflection point was significantly lower when comparing the pressure/oxygenation and pressure/impedance curves. Lung volume changes differed between the ventral and dorsal regions, but did not show a consistent pattern. Optimal recruitment increased the oscillation volume, but the distribution of ventilation was relatively homogeneous along the ventral-dorsal axis.

Conclusions: Lung hysteresis is present in preterm infants with respiratory distress syndrome. Regional differences in lung volume changes and ventilation during high-frequency oscillatory ventilation with lung recruitment are relatively modest and do not follow a gravity-dependent distribution.

Introduction

Despite the increasing use of early nasal continuous positive airway pressure (nCPAP), many infants with respiratory distress syndrome (RDS) still require invasive mechanical ventilation, an intervention that may cause secondary lung injury and is considered one of the major risk factors for bronchopulmonary dysplasia ^{1;2}. Animal studies have identified alveolar overdistention (volutrauma) and collapse (atelectrauma) as the major determinants in the development of secondary lung injury ³. The risk for atelectasis is greatest in the (gravity-) dependent lung regions, which may lead to (regional) overdistention in the nondependent regions. Studies in adults with adult respiratory distress syndrome (ARDS) have confirmed these regional differences, but whether this concept also applies to preterm infants with RDS is unknown ⁴.

Animal studies and mathematical models have suggested that secondary lung injury during mechanical ventilation can be minimized by reversing atelectasis via recruitment maneuvers ⁵⁻⁷. Assuming the presence of lung hysteresis (i.e., a difference in lung volume between the inflation and deflation limbs of the pressure volume curve), such a recruitment maneuver will optimize the end-expiratory lung volume and place ventilation on the more compliant deflation limb of the pressure–volume relationship of the lung ^{5;6}. The concept of lung recruitment has been studied mainly in patients with ARDS treated with conventional (tidal) ventilation, with studies showing that lung hysteresis is indeed present in the adult population ^{8;9}. Studies in preterm lambs have suggested that lung hysteresis is present in neonatal RDS as well ^{10;11}. Based on these findings, lung recruitment is also used in preterm infants with RDS treated with open-lung high-frequency oscillatory ventilation (HFOV), but to date no study has confirmed the presence of lung hysteresis in this specific group of patients.

The main reason for this gap in the knowledge of lung physiology in preterm infants with RDS is the lack of a reliable non invasive bedside tool for measuring changes in lung volume. This also explains why most neonatologists use oxygenation as an indirect marker for lung volume during open-lung HFOV ¹². Electrical impedance tomography is a novel non invasive bedside monitoring technique capable of continuously measuring global and regional changes in lung impedance, which correlate well with intra thoracic changes in air content and ventilation ^{13;14}. Recent studies have shown that electrical impedance tomography is feasible in non sedated preterm infants as well ^{15;16}. The aim of the present study was to monitor the global and regional changes in lung volume and ventilation during oxygenation-guided open-lung HFOV in preterm infants with RDS. We hypothesized that lung hysteresis is present in preterm infants with RDS, and that the changes in lung volume and ventilation during recruitment show regional differences.

Methods

The study was performed in the neonatal intensive care unit of the Emma Children's Hospital, Academic Medical Center (Amsterdam, the Netherlands), where preterm infants (gestational age <37 weeks) with a suspected diagnosis of RDS and failing nCPAP are treated with open-lung HFOV. Infants were included in the study if HFOV was started within 72 hours after birth and written informed consent was obtained from both parents. Exclusion criteria were congenital anomalies, severe circulatory shock, or persistent pulmonary hypertension of the newborn. The study was approved by the hospital's Institutional Review Board.

Ventilation Protocol

HFOV was delivered with a Sensormedics 3100A oscillator (Cardinal Health, Yorba Linda, California) in combination with a protocolized and individualized open-lung ventilation strategy. This ventilation strategy aims to minimize lung injury by recruiting and stabilizing collapsed alveoli with the lowest possible airway pressure, using oxygenation as an indirect marker for lung volume¹². The feasibility and safety of this ventilation strategy was previously described in a large cohort of preterm infants with RDS¹². Following intubation, HFOV was started at a continuous distending pressure (CDP_{st}) of 6-8 cmH_2O , a pressure amplitude resulting in visible oscillation of the chest and a frequency of 10 Hz, with an inspiration time of 33%. The CDP was increased in a stepwise manner (steps of 1-2 cmH_2O) at 2- to 3-minute intervals until oxygenation no longer improved or the fractional inspired oxygen (FiO_2) was ≤ 0.25 , with a transcutaneous oxygen saturation (SpO_2) of 86%-94% (opening pressure, CDP_o). Next, the CDP was decreased in steps of 1-2 cmH_2O until oxygenation deteriorated, indicating alveolar/saccular collapse (closing pressure, CDP_c). Finally, the lung was recruited once more with the known CDP_o and then stabilized with a CDP value 2 cmH_2O above the CDP_c (optimal pressure, CDP_{opt}). The pressure amplitude and frequency were kept constant during the recruitment procedure. All patients were ventilated in the supine position and were not sedated or paralyzed during the recruitment procedure.

Electrical Impedance Tomography Measurements

Before intubation, 16 hand-trimmed electrocardiography electrodes (BlueSensor, BRS-50-K; Ambu Inc, Linthicum Heights, Maryland) were placed equidistantly on the thorax circumference of the newborn just above the nipple line and connected to the Goettingen Goe-MF II electrical impedance tomography system (CareFusion, Hoechberg, Germany). Repetitive electrical currents (5 mA, 100 kHz) were injected in rotation (scan rate, 44 Hz) through adjacent electrode pairs, and voltage changes were measured with all other passive electrode pairs. A back-projection algorithm generated, compared with a reference state, a 32 x 32 matrix image of local relative impedance changes. Continuous

online recording of impedance changes and airway pressure measured at the Y-piece was started as soon as the patient was connected to the HFOV unit, using Veit software (Care-Fusion). Off-line electrical impedance tomography data analysis was done using AUSPEX version 1.6 (VUMC, Amsterdam, The Netherlands).

Pressure/Impedance Relationship

At the start of the analysis, a 30-second reference period was selected from a stable part of the electrical impedance tomography recording at CDP_{st} . All subsequent impedance recordings were referenced to this initial recording, creating a relative impedance change (ΔZ). Following each pressure step, the relative ΔZ was calculated by selecting a stable 30-second period just before the next pressure step and averaging all unfiltered impedance values within that period. To allow for intersubject comparison, the impedance changes were normalized, setting the relative ΔZ at CDP_{st} and CDP_o at 0 and 100%, respectively. Using the absolute pressure steps and the concomitant changes in normalized ΔZ , the inflation and deflation limbs were plotted for all individual patients. Next, the inflation and deflation curves were fitted according to the model described by Venegas et al ¹⁷. First, modelling was done using the absolute pressure changes. Based on these equations, the lower inflection point and the upper inflection point were calculated for both the inflation and deflation limbs of each individual patient, but these pressure points were used for further analysis only if they were within the pressure range used during the actual recruitment procedure. Next, modelling according to Venegas et al was repeated using the normalized pressure, setting CDP_{st} and CDP_o at 0 and 100%, respectively. Predefined 10% pressure steps from 0 to 100% during inflation and from 100% to 0% during deflation were then entered into each individual equation, and the resulting ΔZ values from all patients were averaged for each pressure step. Using all pressure/ ΔZ pairs, the summarized inflation and deflation curves were fitted, and the lower inflection points and upper inflection points, expressed as mean percentage of inflation pressure, were calculated.

The foregoing described analysis was performed using the global, ventral, and dorsal ΔZ values obtained in the whole electrical impedance tomography scan area, as well as in the ventral and dorsal halves of the scan, respectively. To assess possible regional differences in the lower inflection point and upper inflection point, comparative analyses were done between ventral and dorsal values. In addition, the contribution of each of these regions in the total recruited lung volume, defined as the normalized ΔZ at CDP_o , was analyzed.

Ventilation Analysis

To assess the changes in oscillation volume before and after the recruitment procedure, a stable 30-second period was selected at CDP_{st} and CDP_{opt} and referenced to the average ΔZ in that same period. Next, the ΔZ signal was band passfiltered, leaving only

ΔZ changes that occurred in a frequency of $600 \pm 15/\text{minute}$ (10 Hz). By selecting the peaks and troughs of this signal, the oscillatory amplitude was calculated and averaged for the 30-second period. The change in oscillation amplitude between CDP_{st} and CDP_{opt} , expressed as a percentage, was calculated for each patient.

To evaluate the effect of lung recruitment on regional distribution of the oscillatory ΔZ , functional electrical impedance tomography images were generated using the SD of the impedance time course of each individual pixel within the 32×32 matrix at both CDP_{st} and CDP_{opt} ¹⁸. The SD of ΔZ was normalized within each pixel by setting the sum of all pixels at 100%. Next, the total ΔZ in 32 horizontal slices was calculated for each patient, with slice 1 being the most ventral part and slice 32 the most dorsal part. The averaged ΔZ for each slice was then plotted, and the area under curve (AUC) for the ventral region (slices 1-16) and the dorsal region (slices 17-32) were calculated. The geometrical centers (AUC ventral = dorsal) at CDP_{st} and CDP_{opt} were calculated and compared as well.

Analysis

Data on ventilator setting and preductal SpO_2 were collected at the start of lung recruitment and before each change in CDP. To assess the severity of lung disease at the start of ventilation, a modified oxygenation index ($\text{CDP} \times \text{FiO}_2/\text{SpO}_2$) was calculated. The changes in oxygenation, expressed as $\text{SpO}_2/\text{FiO}_2$, were analyzed the same way as the ΔZ data, which provided individual plots of the pressure/oxygenation curve, lower inflection points and upper inflection points by the model of Venegas et al, and a summed inflation and deflation limb based on normalized changes in oxygenation and pressure¹⁷. These results were compared with the data obtained from the electrical impedance tomography analysis.

Statistical analyses were performed using GraphPad Prism 5.0 (Graphpad Software, San Diego, California) and SPSS version 16.0 (SPSS Inc, Chicago, Illinois). Depending on their distribution, data were expressed as mean \pm SD or SEM, or as median with IQR. Nonlinear regression was used to fit the inflation and deflation limbs according to the model of Venegas et al¹⁷. Comparative analyses were performed using the Mann-Whitney or Wilcoxon rank-sum test for skewed data and the Student t test for normally distributed data. A *P* value $< .05$ was considered statistically significant.

Results

Fifteen newborn infants completed the recruitment protocol without any complications (Table I). The mean CDP at the start of lung recruitment (CDP_{st}) was $7.9 \pm 1.2 \text{ cmH}_2\text{O}$, with a mean FiO_2 of 0.75 ± 0.27 . The lungs were recruited

Table 1. Patient characteristics

Subject No.	GA (wk)	Weight (g)	5' Apgar Score	Age (hours)	mOI
1	27.6	995	8	3	9.76
2	31.9	1080	7	3	10.63
3	31.4	1415	6	12	9.09
4	29.0	970	10	16	3.48
5	25.3	750	6	3	4.49
6	28.1	760	9	4	4.53
7	26.9	960	9	16	9.52
8	28.0	720	8	3	8.70
9	25.6	790	7	1	12.00
10	28.3	860	8	3	7.74
11	28.7	820	7	33	3.48
12	29.3	970	7	2	10.81
13	29.3	1095	8	2	3.08
14	28.7	1220	8	14	3.45
15	29.6	1000	5	10	5.27
Median	28.7	970	8	3	7.74

Definition of abbreviations: GA = gestational age, mOI = modified oxygenation index at the start of recruitment using the following equation: $CDP \times FiO_2/SpO_2$. CDP = continuous distending pressure, FiO_2 = fractional inspired oxygen, SpO_2 = transcutaneous oxygen saturation

with a mean opening CDP (CDP_o) of 19.0 ± 1.6 cmH₂O, resulting in a significant drop in the mean FiO_2 to 0.24 ± 0.04 ($P < .01$). The mean closing pressure (CDP_c) was 10.5 ± 1.4 cmH₂O, and the mean optimal pressure (CDP_{opt}) was 12.5 ± 1.4 cmH₂O, with a mean FiO_2 of 0.24 ± 0.03 . In all patients, the oscillation frequency was 10 Hz, and the mean pressure amplitude at the start of recruitment was 18.7 ± 2.4 cmH₂O. Both variables did not change during the recruitment procedure.

Pressure/Impedance Relationship

The individual pressure/impedance curves clearly showed the presence of lung hysteresis in all patients with RDS, although the magnitude of this physiological finding differed among patients (Figure 1). The inflation limb could be modelled in all patients, with a mean goodness of fit (R^2) of 0.99 ± 0.01 . A lower inflection point and upper inflection point during inflation were present in 14 and 12 patients, respectively (Table II). Because of insufficient data points for patient 1, the deflation limb could be modelled in 14 patients ($R^2 = 0.98 \pm 0.01$); this modelling showed only an upper inflection point in the majority of infants (Table II). The summed inflation and deflation curve confirmed the presence of lung hysteresis and showed that the lower inflection point and upper inflection point during inflation and the upper inflection point during deflation occurred at a normalized pressure of 18.7%, 93.7%, and 64.8%, respectively, with small variability (Figure 2).

Analysis of the regional changes in ΔZ during lung recruitment showed ventral and dorsal contributions to the maximal recruited volume of 46% (IQR, 44%-56%) and 54% (IQR, 44%-56), respectively. However, on an individual basis, there was no consistent

pattern favouring one of these regions, with 7 infants with a ventral-dorsal ratio at CDP_o of >1 and 8 infants with a ratio <1 (Figure 1). In 10 of the patients (71%), the dorsal lower inflection point during inflation occurred at a higher pressure compared with the ventral region. In addition, in 9 patients (69%), the upper inflection point during deflation

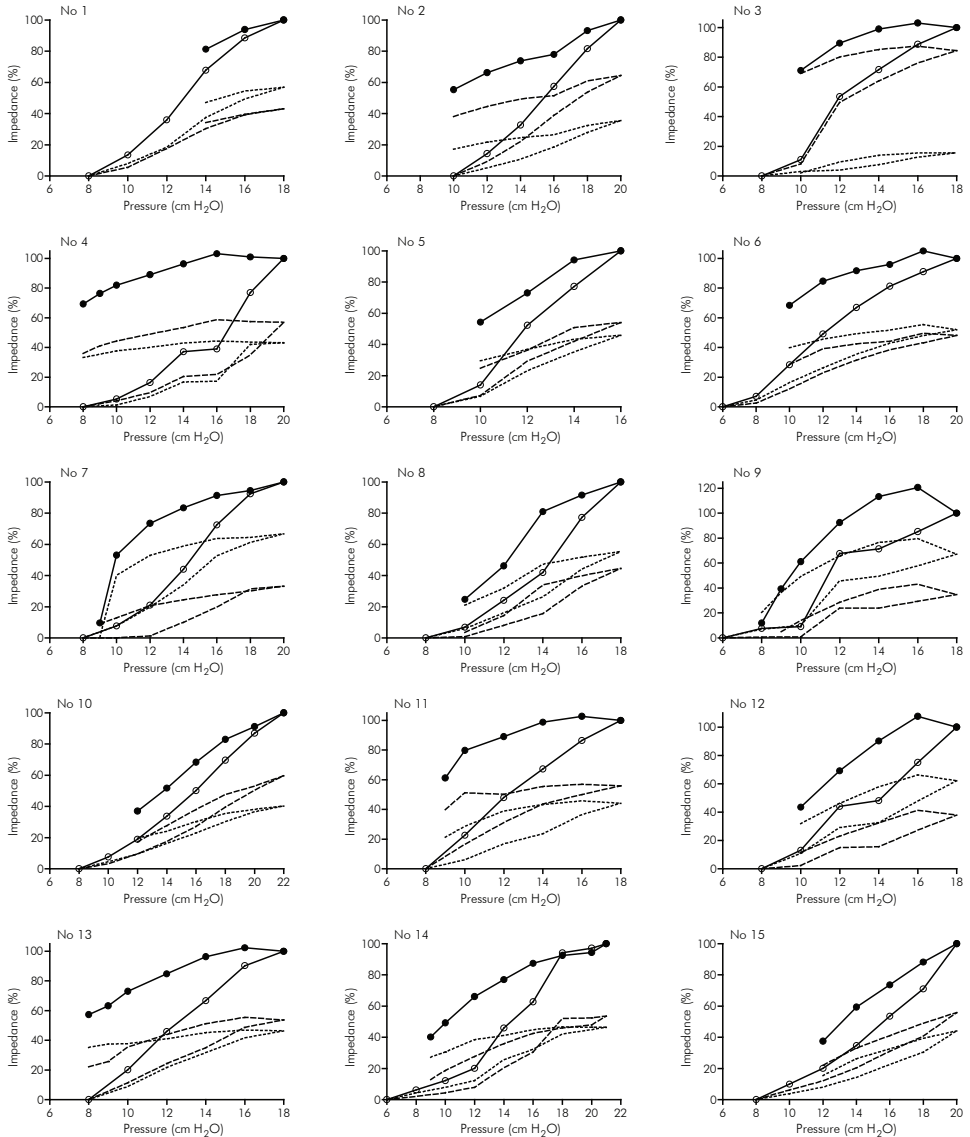


Figure 1 Global and regional pressure/impedance relationship for each individual patient during oxygenation guided open lung high-frequency ventilation. The relative impedance change (ΔZ) is normalized by setting the ΔZ at the start and end of lung recruitment at, respectively, 0% and 100%. Global inflation (open circles) and deflation (closed circles) limbs are presented as solid lines. The ΔZ in the ventral and dorsal regions are depicted as dashed and dotted lines.

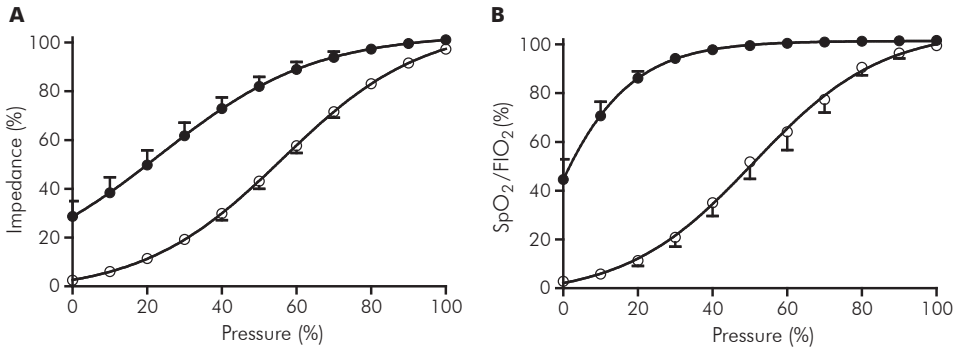


Figure 2 Summarized inflation (open circles) and deflation (closed circles) limb of the pressure/impedance (A) and pressure/oxygenation (B) relationship using normalized data, modeled according to Venegas and colleagues. Data are presented as mean \pm SEM.

occurred earlier in the dorsal region compared with the ventral regions. This pattern was also visible in the summed data on lower inflection point and upper inflection point, but these differences were not statistically significant (Table II).

Pressure/Oxygenation Relationship

In line with the pressure/impedance curves, the plots of the pressure/oxygenation relationship also showed clear hysteresis in all patients (Figure 3). It was interesting to observe that in all but 1 infant, oxygenation showed an (often modest) increase during the first decremental pressure steps. Modelling of the inflation limb ($R^2 = 0.97 \pm 0.03$) and deflation limb ($R^2 = 0.93 \pm 0.07$) was possible in 15 and 11 patients, respectively. The mean lower inflection point during inflation was comparable with the lower inflection point based on the impedance changes. An upper inflection point during inflation was present in 13 patients and tended to be lower compared with the impedance curves (Table II). During deflation, 11 infants had an upper inflection point that was significantly lower compared with the impedance data ($P < .01$) (Table II).

Table 2. Inflection points based on changes in impedance and oxygenation during both inflation and deflation

	LIP _{infl} (cmH ₂ O)	UIP _{infl} (cmH ₂ O)	UIP _{defl} (cmH ₂ O)
SpO ₂ /FiO ₂	11.0 \pm 2.3 (n = 14)	15.4 \pm 2.2 (n = 13)	10.9 \pm 1.9 (n = 11)
Global ΔZ	10.4 \pm 1.8 (n = 14)	17.6 \pm 1.9 (n = 12)	14.7 \pm 2.6 (n = 13)
Ventral ΔZ	10.1 \pm 1.8 (n = 13)	17.5 \pm 1.9 (n = 12)	14.4 \pm 2.4 (n = 13)
Dorsal ΔZ	10.8 \pm 2.0 (n = 13)	17.1 \pm 2.6 (n = 12)	15.0 \pm 3.2 (n = 13)

All values are shown in mean \pm SD; n = number of patients.

Definition of abbreviations: LIP_{infl} = lower inflection point during inflation, UIP_{infl} = upper inflection point during inflation, UIP_{defl} = upper inflection point during deflation, SpO₂ = transcutaneous oxygen saturation, FiO₂ = fractional inspired oxygen, ΔZ = impedance change

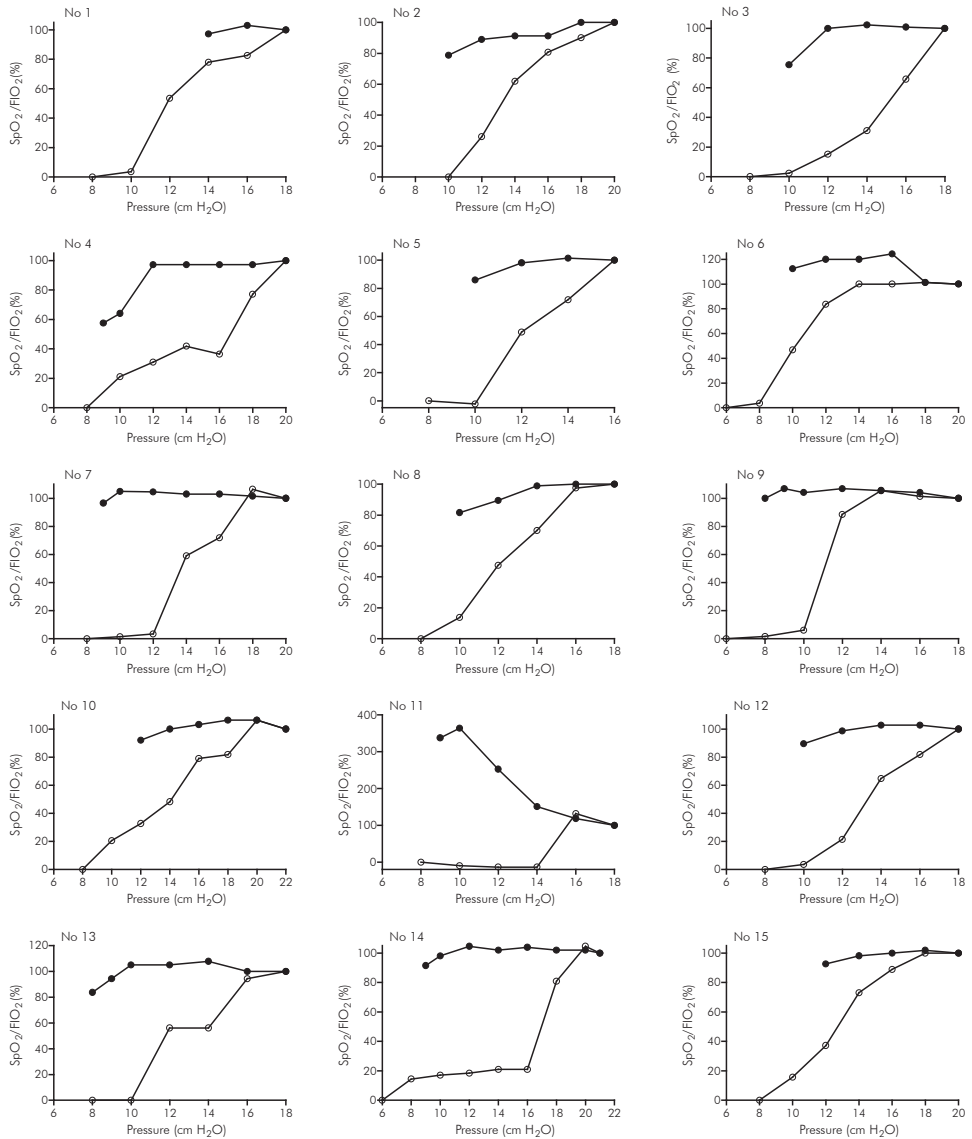


Figure 3 The inflation (open circles) and deflation (closed circles) limbs of the pressure/oxygenation relationship for each individual patient during oxygenation guided open lung high-frequency ventilation. Oxygenation is expressed as transcutaneous oxygen saturation (SpO_2) divided by the fractional inspired oxygen (FiO_2) concentration and normalized by setting the SpO_2/FiO_2 at the start and end of lung recruitment at 0% and 100%, respectively.

Ventilation Data

The median (IQR) increase in oscillation volume before and after lung recruitment was 29.5% (7.5%-44.0%) ($P < .01$). As indicated by the AUC (anterior vs posterior: 49.8% vs 50.3%) and the geometrical center ($50.2\% \pm 4.9\%$), the distribution of oscillatory

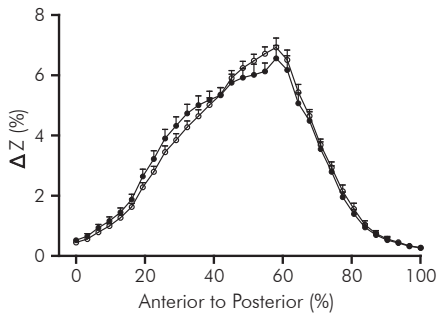


Figure 4 Summarized distribution of the normalized oscillation amplitude (ΔZ in percentage) in 32 anterior to posterior slices of the functional electrical impedance images at the start (closed circles) and optimal pressure (open circles). The ventral-dorsal distance was normalized by setting the most anterior part to 0% and the most dorsal part to 100%. Data are presented as mean \pm SEM.

ventilation at the start of lung recruitment (CDP_{st}) showed a symmetrical pattern between the anterior and posterior lung regions (Figure 4). Following optimal recruitment (CDP_{opt}), there was a small shift in ventilation toward the dorsal lung regions (AUC anterior vs posterior, 46.4% vs 53.6%; geometrical center, $51.5\% \pm 3.2\%$), but this was not statistically significant.

Discussion

Our results indicate that lung hysteresis is present in preterm infants with RDS, and that regional differences in lung volume changes and ventilation during lung recruitment on HFOV are relatively modest and do not show a clear gravity-dependent pattern as is often seen in adult patients with ARDS.

All infants in this study were ventilated with open-lung HFOV using oxygenation as an indirect marker for lung volume. This strategy assumes that an increase in lung volume by alveolar/saccular recruitment will decrease the intrapulmonary shunt fraction and improve oxygenation (SpO_2/FiO_2)^{12;19}. Guided by these changes in oxygenation and assuming the presence of lung hysteresis, the lung volume is optimized for each individual patient through small incremental and decremental pressure steps. By plotting these pressure steps against the changes in oxygenation, we were able to show the presence of lung hysteresis in these patients with RDS. Although this is an important and novel finding, our results should be interpreted with caution, given that oxygenation is an indirect marker for changes in lung volume. For this reason, we also measured lung volume changes with electrical impedance tomography. Animal and human adult studies have shown that the changes in lung impedance during mechanical ventilation are highly correlated with changes in air content seen on computed tomography, and it seems plausible that this would apply to premature infants as well^{13;14}. In line with the oxygenation plots, the individual pressure/impedance curves also showed clear lung hysteresis in all patients, providing strong scientific evidence that this physiological concept also applies to the lungs of preterm infants with RDS.

It has been suggested that the upper inflection point on the inflation limb represents the point after which alveolar recruitment is minimal and a further increase in airway pressure might lead to (regional) overdistention²⁰. Our finding of an upper inflection point in 12 patients might indicate that the majority of infants in this cohort were exposed to possible lung overdistention during recruitment. However, it is important to acknowledge that at the start of the recruitment procedure, the actual upper inflection point is unknown and can be determined only by increasing the airway pressure just past the upper inflection point. At this pressure, alveolar recruitment will be optimal and overdistention will be minimal, especially when airway pressures are immediately reduced on the basis of lung hysteresis. The fact that the normalized upper inflection point occurred at 94% of the inflation pressure with only small variability seems to indicate that this concept can be successfully applied in oxygenation-guided lung recruitment.

It was interesting to observe that during deflation, the upper inflection point based on the oxygenation data was lower than the impedance data. This finding is probably best explained by the fact that, in contrast to impedance, oxygenation can monitor changes in lung volume related only to alveolar/saccular recruitment, not to distention. Assuming that lung volume changes during the final incremental pressure steps and the initial decremental pressure steps are caused mainly by alveolar distention and not recruitment, upper inflection points will be lower when using oxygenation as a marker for lung volume instead of lung impedance.

Another advantage of electrical impedance tomography is its ability to assess changes in lung volume in different regions of interest. Obtaining information on a regional level seems important and relevant, because studies in adult patients with ARDS have shown that lung disease and the response to lung recruitment are often heterogeneous in nature, following a gravity-dependent pattern^{8;14}. The present study shows that changes in lung volume in response to recruitment during HFOV in preterm infants with RDS also demonstrates regional differences, but these differences are relatively small and do not show a consistent gravity dependent pattern. This finding seems to indicate that neonatal RDS in the first 48 hours after birth is a relatively homogeneous lung disease compared with ARDS. Furthermore, the relatively small mass of the upper (ventral) lung regions likely is insufficient to have a gravity-dependent effect on basal (dorsal) regions. Previous studies on the effect of endotracheal tube suctioning on the regional changes in lung volume in preterm infants with RDS also failed to show gravity-dependent changes in lung volume²¹.

Along with lung volume, we also assessed the changes in oscillation volumes during lung recruitment. Despite the fixed delta pressure, our analysis showed a significant increase in oscillation volume between the start of lung recruitment and the optimal position on the deflation limb, which seems to support the findings of animal and mathematical studies of optimal lung compliance on the deflation limb of the pressure/volume curve^{5;11;21}.

In this study, we also analyzed the distribution of oscillation volume between the ventral and dorsal lung regions. Although there was a slight shift toward the dorsal region after lung recruitment, the overall distribution of ventilation appeared to be homogeneous. This is in contrast to the findings of adult experimental and human studies, which show a more heterogeneous ventilation distribution^{14;22}. The latter was also found in a recent study in conventionally ventilated surfactant-deficient newborn piglets²¹. Besides differences in body size, this discrepancy may be explained in part by the fact that lung lavage will result in more heterogeneous lung disease compared with endogenous surfactant deficiency and that ventilation distribution was assessed by tidal ventilation and not (small-volume) high-frequency oscillations.

Tingay et al mapped the deflation limb of the pressure/volume relationship in mostly term, muscle-relaxed newborn infants with various causes of respiratory failure using respiratory induction plethysmography²³. Despite the fact that the characteristics of this cohort were completely different from those of the present study, that study also reported lung hysteresis in the majority of infants. Due to the limitations of respiratory induction plethysmography, the authors were not able to assess the distribution of lung volume or ventilation during lung recruitment.

The present study has several limitations. First, electrical impedance tomography provides information only on a transversal “slice” of the lung. Considering the fact that RDS is a relatively homogeneous lung disease, it is very likely that our electrical impedance tomography findings are representative of the entire lung; however, this might not be the case in more heterogeneous lung disease. Second, although not essential, this study does not provide information on the absolute changes in lung volume. Unfortunately, calibration of the electrical impedance tomography signal to tidal volumes measured at the airway opening is not yet feasible. Third, for reasons of safety, we were not able to fully reconstruct the pressure/volume relationship from residual volume to total lung capacity. However, the presence of a lower inflection point and upper inflection point during inflation and a upper inflection point during deflation in the majority of patients indicates that the clinically relevant parts of the pressure/volume relationship were mapped in the present study.

Besides improving our knowledge on lung physiology in preterm infants with RDS, our study also has some important clinical implications. First, the strong similarity between the pressure/impedance and pressure/oxygenation curves supports the clinical use of oxygenation-guided lung recruitment in preterm infants with RDS. Second, the presence of lung hysteresis emphasizes the need to back-down the CDP at the end of lung inflation to find the lowest possible airway pressure for stabilizing the recruited lung and avoid possible overdistention. Third, the relatively homogenous distribution of lung volume and ventilation changes during recruitment in preterm infants with RDS seems to indicate that body position during this procedure likely is of less importance in these infants than in adult patients with ARDS²⁴. Finally, our findings indicate that mapping of the inflation

and deflation limbs with electrical impedance tomography is feasible at the bedside in non sedated extremely low birth weight infants. This makes electrical impedance tomography a powerful and promising tool for bedside monitoring during newborn ventilation, especially in those cases where oxygenation fails as a monitoring tool for lung volume (ie, extrapulmonary right-to-left shunt).

Reference List

1. Horbar JD, Badger GJ, Carpenter JH, Fanaroff AA, Kilpatrick S, LaCorte M, Phibbs R, Soll RF. Trends in mortality and morbidity for very low birth weight infants, 1991-1999. *Pediatrics* 2002;110:143-151.
2. Jobe AH, Bancalari E. Bronchopulmonary dysplasia. *Am J Respir Crit Care Med* 2001;163:1723-1729.
3. Dreyfuss D, Soler P, Basset G, Saumon G. High inflation pressure pulmonary edema. Respective effects of high airway pressure, high tidal volume, and positive end-expiratory pressure. *Am Rev Respir Dis* 1988;137:1159-1164.
4. Pelosi P, D'Andrea L, Vitale G, Pesenti A, Gattinoni L. Vertical gradient of regional lung inflation in adult respiratory distress syndrome. *Am J Respir Crit Care Med* 1994;149:8-13.
5. Hickling KG. Best compliance during a decremental, but not incremental, positive end-expiratory pressure trial is related to open-lung positive end-expiratory pressure: a mathematical model of acute respiratory distress syndrome lungs. *Am J Respir Crit Care Med* 2001;163:69-78.
6. Rimensberger PC, Cox PN, Frndova H, Bryan AC. The open lung during small tidal volume ventilation: concepts of recruitment and "optimal" positive end-expiratory pressure. *Crit Care Med* 1999;27:1946-1952.
7. van Kaam AH, De JA, Haitsma JJ, Van Aalderen WM, Kok JH, Lachmann B. Positive pressure ventilation with the open lung concept optimizes gas exchange and reduces ventilator-induced lung injury in newborn piglets. *Pediatr Res* 2003;53:245-253.
8. Malbouisson LM, Muller JC, Constantin JM, Lu Q, Puybasset L, Rouby JJ. Computed tomography assessment of positive end-expiratory pressure-induced alveolar recruitment in patients with acute respiratory distress syndrome. *Am J Respir Crit Care Med* 2001;163:1444-1450.
9. Demory D, Arnal JM, Wysocki M, Donati S, Granier I, Corno G, Durand-Gasselien J. Recruitability of the lung estimated by the pressure volume curve hysteresis in ARDS patients. *Intensive Care Med* 2008;34:2019-2025.
10. Luria O, Kohelet D, Barnea O. Optimizing high-frequency-oscillation ventilation using acoustic parameters of the newborn lung: a feasibility study. *Conf Proc IEEE Eng Med Biol Soc* 2007;2007:1269-72.:1269-1272.
11. Pillow JJ, Sly PD, Hantos Z. Monitoring of lung volume recruitment and derecruitment using oscillatory mechanics during high-frequency oscillatory ventilation in the preterm lamb. *Pediatr Crit Care Med* 2004;5:172-180.
12. De Jaegere A, van Veenendaal MB, Michiels A, van Kaam AH. Lung recruitment using oxygenation during open lung high-frequency ventilation in preterm infants. *Am J Respir Crit Care Med* 2006;174:639-645.
13. Frerichs I, Hinz J, Herrmann P, Weisser G, Hahn G, Dudykevych T, Quintel M, Hellige G. Detection of local lung air content by electrical impedance tomography compared with electron beam CT. *J Appl Physiol* 2002;93:660-666.
14. Victorino JA, Borges JB, Okamoto VN, Matos GF, Tucci MR, Caramez MP, Tanaka H, Sipmann FS, Santos DC, Barbas CS, et al. Imbalances in regional lung ventilation: a validation study on electrical impedance tomography. *Am J Respir Crit Care Med* 2004;169:791-800.
15. Miedema M, Frerichs I, de Jongh FH, van Veenendaal MB, van Kaam AH. Pneumothorax in a Preterm Infant Monitored by Electrical Impedance Tomography: A Case Report. *Neonatology* 2010;99:10-13.
16. van Veenendaal MB, Miedema M, de Jongh FH, van der Lee JH, Frerichs I, van Kaam AH. Effect of closed endotracheal suction in high-frequency ventilated premature infants measured with electrical impedance tomography. *Intensive Care Med* 2009;35:2130-2134.
17. Venegas JG, Harris RS, Simon BA. A comprehensive equation for the pulmonary pressure-volume curve. *J Appl Physiol* 1998;84:389-395.

18. Frerichs I, Hahn G, Hellige G. Gravity-dependent phenomena in lung ventilation determined by functional EIT. *Physiol Meas* 1996;17 Suppl 4A:A149-57.:A149-A157.
19. Mancini M, Zavala E, Mancebo J, Fernandez C, Barbera JA, Rossi A, Roca J, Rodriguez-Roisin R. Mechanisms of pulmonary gas exchange improvement during a protective ventilatory strategy in acute respiratory distress syndrome. *Am J Respir Crit Care Med* 2001;164:1448-1453.
20. Rouby JJ, Lu Q, Vieira S. Pressure/volume curves and lung computed tomography in acute respiratory distress syndrome. *Eur Respir J Suppl* 2003;42:27s-36s.:27s-36s.
21. Dargaville PA, Rimensberger PC, Frerichs I. Regional tidal ventilation and compliance during a stepwise vital capacity manoeuvre. *Intensive Care Med* 2010.
22. Wolf GK, Grychtol B, Frerichs I, van Genderingen HR, Zurakowski D, Thompson JE, Arnold JH. Regional lung volume changes in children with acute respiratory distress syndrome during a derecruitment maneuver. *Crit Care Med* 2007;35:1972-1978.
23. Tingay DG, Mills JF, Morley CJ, Pellicano A, Dargaville PA. The deflation limb of the pressure-volume relationship in infants during high-frequency ventilation. *Am J Respir Crit Care Med* 2006;173:414-420.
24. Galiatsou E, Kostanti E, Svarna E, Kitsakos A, Koulouras V, Efremidis SC, Nakos G. Prone position augments recruitment and prevents alveolar overinflation in acute lung injury. *Am J Respir Crit Care Med* 2006;174:187-197.